

Electron-Mediated Nuclear-Spin Interactions Between Distant NV Centers

A. Bermudez,¹ F. Jelezko,² M. B. Plenio,¹ and A. Retzker¹

¹Institut für Theoretische Physik, Albert-Einstein Allee 11, Universität Ulm, 89069 Ulm, Germany

²Institut für Quantenoptik, Albert-Einstein Allee 11, Universität Ulm, 89069 Ulm, Germany

We propose a scheme enabling controlled quantum coherent interactions between separated nitrogen-vacancy centers in diamond in the presence of strong magnetic fluctuations. The proposed scheme couples nuclear qubits employing the magnetic dipole-dipole interaction between the electron spins and, crucially, benefits from the suppression of the effect of environmental magnetic field fluctuations thanks to a strong microwave driving. This scheme provides a basic building block for a full-scale quantum information processor or quantum simulator based on solid-state technology.

The spins of single dopants in solids are key elements in the development of solid-state quantum-information technologies [1, 2]. In particular, nitrogen-vacancy (NV) colour centers in diamond are promising quantum processors: single defects can be detected using confocal microscopy [3, 4], their spin state can be initialized, manipulated, and readout optically [5–8], and their quantum coherence survives at room temperatures [9]. One of the remaining challenges is to control the spin-spin interactions to perform quantum-logic operations, and major steps along this direction have already been accomplished. The hyperfine coupling between the NV electron spin and the nuclear spins of neighboring impurities (¹³C, ¹⁵N) offers a unique opportunity to build small quantum registers [8, 10, 12–14]. These devices can be scaled up by means of ion implantation techniques, yielding periodic arrays of NV centers [15]. However, the controlled couplings now require longer-range interactions, as provided by optical channels [16], or magnetic dipole-dipole couplings between the electron spins [17].

Although the feasibility of the magnetic-coupling approach has been demonstrated recently [17], fabricated NV arrays often suffer from shorter electron coherence times that affect the fidelity of the quantum gates. From this perspective, ¹⁴N or ¹⁵N nuclear spins would be better-suited qubits due to their longer coherence times, together with the availability of single-shot readout [10]. Unfortunately, the direct nuclear dipole-dipole interaction is negligible, which necessitates the search for alternative schemes to couple the nuclear spins. This letter presents a theoretical proposal for implementing robust quantum gates between two distant nuclear-spin qubits mediated by the long-range dipolar interaction between electron spins. The main idea is to exploit the long nuclear coherence times for storage, and to use the electronic degrees of freedom as a quantum bus that mediates the nuclear spin interaction. Such a general scheme can be applied to different setups, and has also been proposed for quantum-Hall systems [11]. Active control of the spins via microwave fields allows reaching high fidelities, even in the presence of the magnetic noise associated to the complex mesoscopic environment of solid-state systems. In fact, the nuclear driving acts as a continuous decoupling mechanism [18] that minimizes the effects of the noise, and provides a new tool in addition to pulsed techniques [19].

The model.— We consider two NV defects $j = 1, 2$, whose unpaired electrons form a spin-triplet ground state $S_j = 1$, and

focus on ¹⁴N with a nuclear spin $I_j = 1$. The Hamiltonian that describes each NV center is $H_j = H_j^{(e)} + H_j^{(n)} + H_j^{(e-n)}$,

$$\begin{aligned} H_j^{(e)} &= D_j \left((S_j^z)^2 - \frac{1}{3} S_j^2 \right) + g_e \mu_B \mathbf{B} \cdot \mathbf{S}_j, \\ H_j^{(n)} &= -P_j \left((I_j^z)^2 - \frac{1}{3} I_j^2 \right) - g_n \mu_N \mathbf{B} \cdot \mathbf{I}_j, \\ H_j^{(e-n)} &= A_j^{\parallel} S_j^z I_j^z + \frac{1}{2} A_j^{\perp} (S_j^+ I_j^- + S_j^- I_j^+), \end{aligned} \quad (1)$$

where $\mathbf{S}_j, \mathbf{I}_j$ are the electronic and nuclear spin-1 operators, and $S_j^{\pm} = S_j^x \pm i S_j^y$, $I_j^{\pm} = I_j^x \pm i I_j^y$ the usual ladder operators. Here, $D_j(P_j)$ stands for the zero-field splitting of the electronic (nuclear) ground state, \mathbf{B} is an external magnetic field, $\mu_B(\mu_N)$ is the Bohr (nuclear) magneton, and $g_e(g_n)$ is the electron (nuclear) g-factor. The electron-nuclei interaction is quantified by the hyperfine longitudinal (transverse) coupling $A_j^{\parallel}(A_j^{\perp})$. The present discussion is focused on a single pair of closely-spaced NV centers, and we use the realistic parameters of the experiment in [17]. We emphasize, however, that this scheme can be extended to arrays of implanted NV centers, provided that their distance is small enough. Let us also remark the hierarchy of couplings, $D_j \gg P_j \gtrsim A_j^{\parallel}, A_j^{\perp}$, and $g_e \mu_B \gg g_n \mu_N$ (see Table I, where $\hbar = 1$). Finally, we introduce the secular dipole-dipole interaction between the electron spins

$$H_{12}^{(e-e)} = J_{12} (3S_1^z S_2^z - \mathbf{S}_1 \cdot \mathbf{S}_2), \quad (2)$$

where $J_{12} = g_e^2 \mu_B^2 (1 - 3 \cos^2 \theta_{12}) / 2cr_{12}^3$ in gaussian units, r_{12} is the distance between the NV centers, $\cos \theta_{12} = \mathbf{e}_z \cdot \mathbf{r}_{12} / r_{12}$, and c is the speed of light. For the distances reached in the experiment, $r_{12} \approx 10$ nm, the dipolar coupling $J_{12} \approx 70$ kHz is the smaller energy scale in the problem. As mentioned above, the magnetic dipole-dipole interaction between the nuclear spins is completely negligible since $(g_n \mu_N / g_e \mu_B)^2 \approx 10^{-8}$, and an indirect mechanism for the nuclear coupling is thus required.

Effective static interactions.— In Fig. 1(a), we represent schematically the process leading to nuclear spin-spin interactions. The hyperfine interaction couples the nuclear to the electronic spins of each NV center, which are in turn coupled through the magnetic dipole-dipole interaction. Therefore, one may use the electrons as a bus to mediate the nuclear coupling. A naive estimate of this coupling follows from Fig. 1(b), where we represent the energy spectrum of $H_0 = \sum_j (H_j^{(e)} + H_j^{(n)}) + H_{12}^{(e-e)}$. Due to the energy-scale hierarchy in Table I, the levels are clustered in manifolds determined by the electronic spins $|m_1, m_2\rangle_e$. The dynamics within the ground-state manifold, $|0, 0\rangle_e$, corresponds

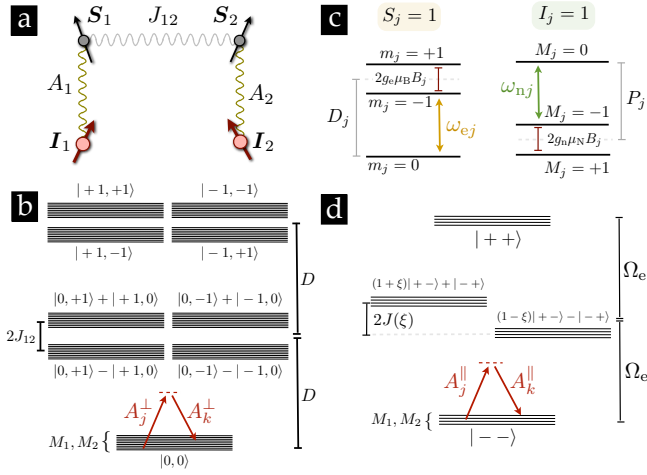


Figure 1. Effective nuclear spin-spin interaction. (a) Schematic diagram of the electron-mediated interaction between the nuclear spins, which exploits the magnetic dipolar interaction and the local hyperfine coupling. (b) Diagram of the energy levels of the two NV centers. Since D_j is the largest energy scale, the energies are clustered in manifolds determined by the electronic spin. The transverse part of the hyperfine coupling A_j^\perp induces transitions between different manifolds, and mediates an effective XX interaction between the nuclear spins. (c) Schematic diagram of the Zeeman splitting for the electronic and nuclear energy levels. By carefully selecting the microwave frequencies, we drive a particular electronic and nuclear transition. (d) Energy levels of the driven Hamiltonian. For very strong driving Ω_e , the electronic spin in the lowest manifold is $|-\rangle \propto |0\rangle - |-1\rangle$. The hyperfine coupling A_j^\parallel induces virtual transitions to the excited manifold, split by the dipolar interaction and the inhomogeneous broadening, and leads to an effective ZZ interaction.

to nuclear spin flips $|M_1, M_2\rangle_n \rightarrow |M'_1, M'_2\rangle_n$, with $M_j, M'_j = 0, \pm 1$, and follows from second-order processes where the hyperfine coupling virtually populates states from the excited manifold. Therefore, a crude estimate of the dynamics is $H_{\text{eff}} \approx J_{\text{eff}} I_1^+ I_2^- + \text{H.c.}$, where $J_{\text{eff}} \propto (A_1^\perp A_2^\perp)/D$. A more careful Schrieffer-Wolff-type calculation takes into account the two possible channels, symmetric or anti-symmetric, which lead to the destructive interference of this coupling $J_{\text{eff}} \propto (A_1^\perp A_2^\perp)/D - (A_1^\perp A_2^\perp)/D$. It is precisely the role of the magnetic dipole-dipole interaction to split these channels, suppressing the perfect destructive interference, and leading to

$$H_{\text{eff}}^{\text{xx}} = J_{\text{eff}}^{\text{xx}} (I_1^+ I_2^- + I_1^- I_2^+) - \sum_j P_j (I_j^z)^2, \quad J_{\text{eff}}^{\text{xx}} = \frac{2A_1^\perp A_2^\perp}{D^2} J_{12}. \quad (3)$$

This Hamiltonian describes the *flip-flop interaction* between the ^{14}N nuclei leading to an exchange of the spin excitations.

In Fig. 2(a), we present a scheme for the electron-mediated gate between two NV nuclei based on Eq. (3), referred as the nuclear XX gate. The initialization yields the state $|\psi_0\rangle = |\phi_e\rangle \otimes |\varphi_n\rangle = |0, 0\rangle_e \otimes |0, 1\rangle_n$, where electrons belong to the ground-state manifold of Fig. 1(b), and the dynamics of the spin excitation is determined by virtual electron spin-flip processes. In Fig. 2(c), we study numerically the accuracy of the effective Hamiltonian (3), which is compared to the exact evolution under the total Hamiltonian (1)-(2). One observes that

the electron state remains in the ground-state, whereas there is a periodic exchange of the spin excitation between the nuclei. The remarkable agreement of both predictions justifies the validity of the effective nuclear spin-spin Hamiltonian in Eq. (3). Unfortunately, the parameters in Table I yield a vanishingly-small coupling $J_{\text{eff}}^{\text{xx}} \approx 0.1\text{Hz}$, which is far too slow to produce any observable coherent coupling between the nuclei. Even if not of practical use, the above derivation gives a neat account of the mechanism of electron-mediated interactions, and will help us in understanding how to raise the interaction strength.

A possibility to overcome this problem is to apply a magnetic field, such that the Zeeman shift reduces $D \rightarrow D - g_e \mu_B B$, thus enhancing $J_{\text{eff}}^{\text{xx}}$. Yet, one faces two important problems: *i)* In general, the axes of the NV centers are not aligned, and each electronic spin experiences a different Zeeman shift. For the large fields required, this inhomogeneity might exceed the dipolar coupling, and thus spoil the scheme. *ii)* The dephasing exerted by the environment would have a contribution that ruins the coherence of the interaction. We demonstrate below that there is a different approach that overcomes both problems simultaneously, and yet enhances the nuclear spin interaction: *continuous microwave driving* [18].

Effective driven interactions.— We discuss now the effects of a continuous microwave field that drives both the electronic and nuclear spins. The effect of the driving is two-fold: *i)* By addressing each NV center with different microwave fields, one can independently tune their frequencies so that they become resonant with a particular transition. This allows us to overcome the problems associated with both the inhomogeneous broadening, and the different Zeeman shifts. Moreover, this can be used for single addressing of NV's, especially when combined with magnetic gradients. *ii)* By tuning the microwave frequency on resonance with the transition, one introduces a new energy scale that governs the system, namely the Rabi frequency. This parameter can be tuned by controlling the microwave power, allowing us to enhance J_{eff} .

Let us consider the Zeeman effect associated to $B = 30\text{G}$ in Fig. 1(c). By setting the microwave frequencies to $\omega_{e_j} = D_j - g_e \mu_B B_j$, $\omega_{n_j} = P_j - g_n \mu_N B_j$, one resonantly drives the transitions between the electronic and nuclear levels $m_j = 0 \leftrightarrow -1$, $M_j = 0 \leftrightarrow -1$. These driving terms can be written as

$$H_d(t) = \sum_j \Omega_e \sigma_j^x \cos \omega_{e_j} t + \Omega_n \tau_j^x \cos \omega_{n_j} t, \quad (4)$$

where the Rabi frequencies of the electronic and nuclear transitions are Ω_e, Ω_n , and the electronic and nuclear Pauli matrices σ_j^x, τ_j^x . In the interaction picture with respect to $H_{0,1} = \sum_j D_j (S_j^z)^2 - P_j (I_j^z)^2 + g_e \mu_B B_j S_j^z - g_n \mu_N B_j I_j^z$, one can neglect the rapidly oscillating terms associated to the transverse part of Zeeman shifts, and the hyperfine coupling. This rotating wave approximation is justified for the parameters shown in Table I. Additionally, we consider two NV centers with different axes, which allows us to neglect the transverse part of the magnetic dipole coupling. For weak-enough driving, we arrive at the the total *driven Hamiltonian*

$$H_0 = \sum_j \left(\frac{1}{2} \Omega_e \sigma_j^x + \frac{1}{2} \Omega_n \tau_j^x \right) + 2J_{12} S_1^z S_2^z, \quad H_1 = \sum_j A_j^\parallel S_j^z I_j^z. \quad (5)$$

Table I. Specific values of the coupling strengths

D_j	P_j	$A_j^ , A_j^\perp$	J_{12}	$g_e \mu_B$	$g_n \mu_N$	B	Ω_e	Ω_n	$J_{\text{eff}}^{\text{xx}}$	$J_{\text{eff}}^{\text{zz}}$
2.87 GHz	5.04 MHz	2.1, 2.3 MHz	70 kHz	2.8 MHz · G ⁻¹	0.31 kHz · G ⁻¹	30 G	15 MHz	1 kHz	0.1 Hz	0.1 kHz

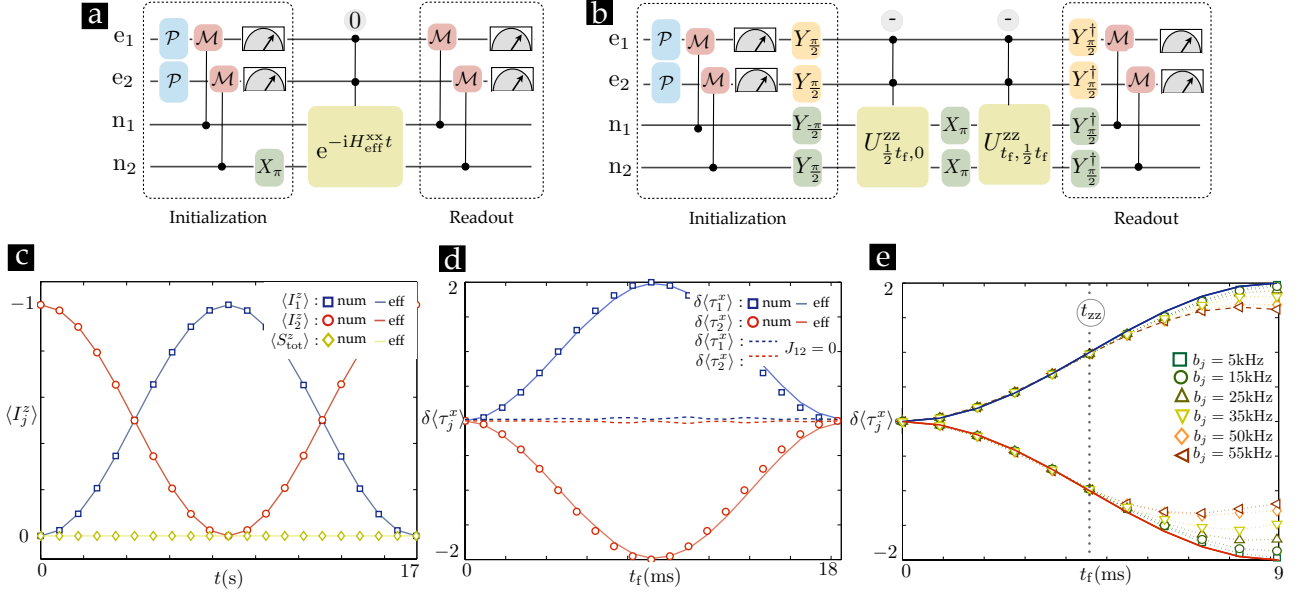


Figure 2. **Nuclear quantum gate between two NV centers:** Scheme for the initialization, evolution, and read-out of the effective $J_{\text{eff}}^{\text{xx}}$ interaction in (a), and $J_{\text{eff}}^{\text{zz}}$ interaction in (b). Here, $X_{j,\phi} = \exp(i\phi\tau_j^x/2)$, $Y_{j,\theta} = \exp(i\theta\tau_j^y/2)$ represent finite pulses, and $\mathcal{P}(\mathcal{M})$ stand for the electron (nuclear) spin polarization. (c) Comparison between the effective dynamics under the Hamiltonian (3) and the exact time evolution under Eqs. (1)-(2) for the $J_{\text{eff}}^{\text{xx}}$ nuclear interaction. The expectation values represented correspond to the nuclear spin $\langle I_j^z \rangle$, and electronic spin $\langle S_{\text{tot}}^z \rangle = \langle S_1^z + S_2^z \rangle$. (d) Comparison between the exact (5) and effective (6) dynamics for the $J_{\text{eff}}^{\text{zz}}$ nuclear interaction, together with an echo scheme that allow us to get rid of the fast single-nuclei dynamics. We represent the nuclear expectation values $\delta \langle \tau_j^x \rangle = \langle \tau_j^x \rangle_{t_f} - \langle \tau_j^x \rangle_{t_0}$. The dotted lines correspond to $J_{12} = 0$, where there is no interaction induced on the nuclei. (e) Performance of the ZZ-gate in the presence of different strengths of the electron dephasing noise $b_j = \{5, 15, 25, 35, 50, 55\}$ kHz, where the nuclear noise is $B_j = 0.1b_j$. The corresponding Ramsey decoherence times are roughly $T_{2e} \approx \{0.2, 0.07, 0.04, 0.03, 0.02, 0.018\}$ ms, $T_{2n} = 0.1T_{2e}$.

We stress that these approximations are justified by the parameters in Table I, and supported by numerical simulations.

We derive now the electron-mediated nuclear spin interactions starting from Eq. (5). We note that there is again a hierarchy in the couplings $\Omega_e \gg A_j^|| \gg J_{12} \gg \Omega_n$, which leads to the clustering of energy levels shown in Fig. 1(d). By considering the electron ground-state, the nuclear spins can interact through virtual electron spin-flips to the excited manifolds. In this driven regime, it is the longitudinal hyperfine coupling $A_j^||$ which induces such virtual transitions. A Schrieffer-Wolff-type calculation yields the nuclear Hamiltonian

$$H_{\text{eff}}^{\text{zz}} = J_{\text{eff}}^{\text{zz}} \tau_1^z \tau_2^z + \sum_j \Omega_n \tau_j^x - \frac{1}{4} A_j^|| \tau_j^z, \quad J_{\text{eff}}^{\text{zz}} = \frac{-A_1^|| A_2^||}{8\Omega_e} \left(\frac{J_{12}}{\Omega_e} + 2\xi \right), \quad (6)$$

where we considered the inhomogeneous broadening of the hyperfine couplings $\xi = 2[(A_2^||)^2 - (A_1^||)^2]/\Omega_e J_{12}$. This Hamiltonian is an *Ising magnetic interaction* between the nuclear spins, which are additionally subjected to a transverse field due to the driving, and a longitudinal field due to the hyperfine coupling. As advanced previously, we have been able

to enhance the electron-mediated nuclear interaction, which becomes $J_{\text{eff}}^{\text{zz}} \approx 0.1$ kHz for the parameters in Table I. Remarkably, the strength of the nuclear spin interaction has increased by three orders of magnitude $J_{\text{eff}}^{\text{zz}} \approx 10^3 J_{\text{eff}}^{\text{xx}}$.

In Fig. 2(b), we schematically describe the necessary ingredients for the nuclear ZZ gate. The initialization consists of the electron (nuclear) spin polarization $\mathcal{P}(\mathcal{M})$, together with single-spin gates. \mathcal{P} is obtained by the optical pumping cycle available for NV centers [5, 6], whereas \mathcal{M} is based on the techniques developed for the nuclear single-shot measurement [10], followed by the electron state-dependent fluorescence [5, 6]. Once polarized, $|0,0\rangle_e \otimes |0,0\rangle_n$, one applies unitary gates based on microwave pulses of different duration, $Y_{j,\frac{\pi}{2}} = (\mathbb{I} + i\tau_j^y)$, $Y_{j,-\frac{\pi}{2}} = (\mathbb{I} - i\tau_j^y)$ (also for the electron spin), which lead to $|\psi_0\rangle = |--\rangle_e \otimes |--\rangle_n$. The evolution of this state is dictated by the interaction-picture Hamiltonian (6), which leads to $U_{t_2,t_1}^{\text{zz}} = e^{-iH_{0,1}t_2} e^{-iH_{\text{eff}}^{\text{zz}}(t_2-t_1)} e^{iH_{0,1}t_1}$. Due to the longitudinal field, and the additional contributions of $H_{0,1}$, the simple periodic exchange of the nuclear spin excitation shall be accompanied by fast oscillations. In order to observe

neatly the effect of the interaction, one may perform a spin-echo sequence, such that the nuclear spins are inverted at half the gate time by a microwave pulse $X_{j,\pi} = i\tau_j^x$. In this case, the fast single-nuclei oscillations refocus after the spin-echo period t_f , and one observes solely the effect of the interaction. In Fig. 2(d), we compare the effective description (6) to the Hamiltonian (5), which display a clear agreement. In particular, when the echo period matches twice the ZZ-gate time $t_f = 2t_{zz} = \pi/2J_{\text{eff}}^{zz} \approx 9\text{ms}$, one finds a perfect excitation exchange $\langle \tau_1^x \rangle : -1 \rightarrow +1$, $\langle \tau_2^x \rangle : +1 \rightarrow -1$. Note that for $J_{12} = 0$, this effect is completely absent. Finally, considering $t_f = t_{zz}$, and setting the echo pulse along the y-axis, the dynamics generates an entangled nuclear state $|\psi_0\rangle = |--\rangle_e \otimes |-y+y\rangle_n \rightarrow |\psi_f\rangle = |--\rangle_e \otimes (|-y+y\rangle_n + |+y-y\rangle_n)/\sqrt{2}$. Once the gate has been performed, the nuclear operators $\langle I_j^z \rangle$, $\langle \tau_j^x \rangle$ must be measured. Since the state-dependent fluorescence is particular to the electron spins, one should map the nuclear information onto the electrons, and then measure. This can be achieved in a quantum non-demolition fashion by using a microwave on an electron-spin transition conditioned to the nuclei [10].

Decoupling from decoherence.- So far, our discussion has focused on the idealized situation of isolated NV centers. However, every quantum system is inevitably coupled to an environment that degrades its coherence. This phenomenon, known as *decoherence*, must be seriously accounted for in solid-state materials, where the system-environment coupling is usually strong. In the particular case of NV centers, the major source of decoherence is the coupling to other impurity spins, such as single substitutional nitrogen electron spin (P1 center) in type Ib diamond [21], or ^{13}C isotopes in type IIa [8]. The microscopic description of the spin bath is an intricate many-body problem, and is a current subject of intense research. Here, we use a phenomenological model of the bath that yields a fluctuating magnetic field shifting the resonance frequencies. Due to the spin interactions, this effective field is modeled as a stochastic Ornstein-Uhlenbeck process [19, 22]

$$H_{\text{noise}} = \sum_j \left(b_j(t) S_j^z + B_j(t) I_j^z \right), \quad (7)$$

where $b_j(t), B_j(t)$ are random processes with autocorrelation $\langle b_j(t) b_j(0) \rangle = b_j^2 e^{-r_j t}$, $\langle B_j(t) B_j(0) \rangle = B_j^2 e^{-R_j t}$, where b_j^2, B_j^2 represent variance of the zero-mean gaussian distributions, and r_j, R_j the inverse of their correlation times. In particular, the decoherence time of an electronic (nuclear) Ramsey experiment is given by $T_{2e} = 1/b_j$ ($T_{2n} = 1/B_j$). By considering the particular time-dependence of these stochastic processes, we numerically integrate the noisy dynamics, and average for

$N = 10^3$ realizations of the random process. This allows us to study the effects of decoherence on the gate.

For the slow XX gate (Fig. 2(a)), the limiting factor is the nuclear dephasing time, which can attain values of $T_{2n} \approx 10\text{ms}$. Even for the purest samples, the coherence of the gate is completely lost much before the target time $t_{xx} \approx 4.5\text{s}$ is reached. Therefore, the performance of this gate is extremely poor. For the fast ZZ gate (Fig. 2(b)), not only the nuclear-spin dephasing, but also the electron-spin dephasing limit the gate accuracy. In the dressed-state basis (see Fig. 1(d)), the electron dephasing tries to induce a transition between the different manifolds, introducing additional noise in the nuclei. However, due to the strong driving Ω_e , these processes are partially suppressed. Additionally, a sufficiently strong nuclear driving, $\Omega_n \gg B_j, (b_j A_j^{\parallel} / \Omega_e)$, provides an additional decoupling mechanism that enhances further the gate performance. In Fig. 2(e), one observes the announced decoupling, since the gate performance at the target time $t_{zz} \approx 4.5\text{ms}$ is extremely good even for shorter electronic coherence times ranging from $T_{2e} \approx 0.1\text{ms}$ to $T_{2e} \approx 50\mu\text{s}$. Due to the decoupling mechanism, the gate accuracy will actually be limited by the decay times T_{1e} . Moreover, at this time scale, energy will be pumped into the system by the continuous driving. However, note that this limitation can be overcome since T_{1e} can be increased by orders of magnitude by cooling. Accordingly, one can achieve high fidelities.

Let us finally note that the effective decoupling mechanism presented here can also be used to improve the electron-spin gates based on the direct dipole interaction [17]. In that case, the role of the microwave driving is to prolong dephasing times and to bring the two dressed electronic transitions to resonance to overcome the inhomogeneous broadening.

Conclusions and outlook.- We have demonstrated the feasibility for engineering electron-mediated spin-spin interactions between the nuclei of two NV-centers. By continuous microwave driving, this scheme allows us to decouple from the electronic and nuclear dephasing sources, and increase the effective interactions by three orders of magnitude thus achieving $J_{\text{eff}}^{zz} \approx 0.1\text{kHz}$ for distances of existing pairs of NV-centers [17]. This scheme opens the possibility for the realization of quantum information processors, quantum simulators and quantum-sensors [23] on the basis of NV-centers in diamond. Finally, we would like to stress the generality of this scheme, which can be applied to other solid-state technologies that are candidates for quantum-information processing.

Acknowledgements.- This work was supported by the EU STREP projects HIP, PICC, and by the Alexander von Humboldt Foundation. We thank J. Cai for useful discussions.

[1] J. R. Weber, et al. *Proc. Natl. Acad. Sci.* **107**, 8513 (2010).
 [2] T. D. Ladd, et al. *Nature* **464**, 45 (2010).
 [3] A. Gruber, et al. *Science* **276**, 2012 (1997).
 [4] C. Kurtsiefer, et al. *Phys Rev Lett* **85**, 290 (2000).
 [5] F. Jelezko, et al. *App. Phys. Lett.* **81**, 2160 (2002).
 [6] F. Jelezko, et al. *Phys. Rev. Lett.* **92**, 076401 (2004).
 [7] R. J. Epstein, et al.. *Nat. Phys.* **1**, 94 (2005).

[8] L. Childress, et al. *Science* **314**, 281 (2006).
 [9] G. Balasubramanian, et al. *Nat. Mater.* **8**, 383 (2009).
 [10] P. Neumann, et al. *Science* **329**, 542 (2010).
 [11] V. Privman, I. D. Vagner and G. Kventsel *Phys. Lett. A.* **239**, 141 (1998).
 [12] T. Gaebel, et al. *Nat. Phys.* **2**, 408 (2006).
 [13] P. Neumann, et al. *Science*, **320**, 1326 (2008).

- [14] M. V. Gudurev Dutt, et al. *Science* **316**,1312 (2007).
 [15] J. Meijer, et al. *Appl. Phys. A* **83**, 321 (2006); W. Schnitzler, et al. *Phys. Rev. Lett.* **102**, 070501 (2009); D. M. Toyli, et al. *Nano Lett* **10**, 3168 (2010).
 [16] E. Togan, et al. *Nature* **466**, 730 (2010).; Y. Kubo, et al. *Phys. Rev. Lett.* **105**, 140502 (2010).; A. D. Greentree, et al. *J. Phys.: Condens. Mat.* **18**, S825 (2006).
 [17] P. Neumann, et al. *Nat. Phys.* **6**, 249 (2010).
 [18] N. Timoney, et al. *Nature* **476**, 185 (2011); B. Naydenov, et al. *Phys. Rev. B* **83**, 081201 (2011).
 [19] G. de Lange, et al. *Science* **330**, 60 (2010).
 [20] H. Bluhm, et al. *Nat. Phys.* **7**, 109 (2011).
 [21] R. Hanson, et al. *Science* **320**, 352 (2008).
 [22] V. V. Dobrovitski, et al., *Phys. Rev. Lett.* **102**, 237601 (2009).
 [23] G. Balasubramanian, et al. *Nature* **455**, 648 (2008); J. M. Taylor, et al. *Nat. Phys.* **4**, 810 (2008); J. R. Maze, et al. *Nature* **455**, 644 (2008); L. T. Hall, et al., *Proc. Natl. Acad. Sci.* **107**, 18777 (2010).

I. SUPPLEMENTARY MATERIAL

In the following sections, we provide a detailed discussion of some technical aspects used to derive the main results presented above. In the first section, we derive the effective nuclear Hamiltonians in Eqs. (3)-(6) by means of the so-called Schrieffer-Wolff transformation. Finally, in the second section, we describe the phenomenological model used to study the effects of the decoherence on the nuclear-gate performance.

1. Schrieffer-Wolff transformation and effective nuclear Hamiltonians

In this section, we review the theory of quasi-degenerate perturbation theory as a tool to perform the so-called *adiabatic elimination* of the fast degrees of freedom in a quantum-mechanical system [1]. In particular, this technique allows us to derive the effective spin-spin Hamiltonians for the nuclei.

Schrieffer-Wolff transformation.-We shall assume that the Hamiltonian is of the form $H = H_0 + \lambda V$, where λV is a weak perturbation to the unperturbed Hamiltonian $H_0 = H_A + H_B$. Here, H_A and H_B describe the *slow* and *fast* degrees of freedom

$$H_A|j\alpha\rangle = E_\alpha|\alpha\beta\rangle, \quad H_B|\alpha\beta\rangle = E_\beta|\alpha\beta\rangle, \quad (8)$$

where $|E_\alpha - E_{\alpha'}| \ll |E_\beta - E_{\beta'}|$. Accordingly, the frequencies associated to the $\beta \rightarrow \beta'$ transitions, $\omega_{\beta\beta'} = E_\beta - E_{\beta'}$, are much larger than those of $\alpha \rightarrow \alpha'$, $\omega_{\alpha\alpha'} = E_\alpha - E_{\alpha'}$, and they can be adiabatically eliminated. By performing a canonical transformation $U = e^S$, $S^\dagger = -S$, one constructs an effective Hamiltonian $H_{\text{eff}} = U^\dagger H U$ that only involves the slow degrees of freedom, $P_\beta H_{\text{eff}} P_\beta = H_{\text{eff}}^\beta \delta_{\beta\beta'}$, where $P_\beta = \sum_\alpha |\alpha\beta\rangle\langle\alpha\beta|$. The canonical transformation S , and the effective Hamiltonian H_{eff} , can be constructed to any order of the perturbative parameter λ . This is usually known as the Schrieffer-Wolff transformation in condensed matter [2], although it also arises in a broader context [3, 4]. To second order [1], one finds the following expression

$$\langle\alpha|H_{\text{eff}}^\beta|\alpha'\rangle = (E_\alpha + E_\beta)\delta_{\alpha\alpha'} + \langle\alpha\beta|\lambda V|\alpha'\beta\rangle + \frac{1}{2} \sum_{\alpha''\beta''} \langle\alpha\beta|\lambda V|\alpha''\beta''\rangle \langle\alpha''\beta''|\lambda V|\alpha'\beta\rangle \left(\frac{1}{\omega_{\alpha\alpha''} + \omega_{\beta\beta''}} + \frac{1}{\omega_{\beta\beta''} + \omega_{\alpha'\alpha''}} \right). \quad (9)$$

Since we have fast and slow components $\omega_{\beta\beta''} \gg \omega_{\alpha\alpha''}$, we may expand $(\omega_{\alpha\alpha''} + \omega_{\beta\beta''})^{-1} \approx \omega_{\beta\beta''}^{-1}(1 - \omega_{\alpha\alpha''}/\omega_{\beta\beta''})$ in Eq. (9), which allows us to get an effective Hamiltonian that only acts on the slow degrees of freedom

$$H_{\text{eff}}^\beta \approx P_\beta (H_0 + \lambda V) P_\beta + \lambda^2 \sum_{\beta''} P_\beta \frac{V|\beta''\rangle\langle\beta''|V}{\omega_{\beta\beta''}} P_\beta. \quad (10)$$

In this manuscript, we make use of this canonical transformation to adiabatically eliminate the fast degrees of freedom of the electrons localized around a Nitrogen-vacancy impurity in diamond, and obtain an effective Hamiltonian for the slow ^{14}N nuclei.

Effective nuclear Hamiltonian for the static regime.- According to the above discussion, one should first identify the fast and slow degrees of freedom of the Hamiltonian in Eqs. (1)-(2). Regarding the parameters in Table I, together with the energy levels in Fig. 1(b), it is clear that the fast degrees of freedom correspond to electronic spin flips $\beta = \{m_1, m_2\}$, whereas the slow degrees of freedom involve the nuclei $\alpha = \{M_1, M_2\}$. Besides, the weak perturbation corresponds to the hyperfine interaction, which couples different electronic manifolds. We are interested in the dynamics within the electronic ground-state manifold $\beta = \{0, 0\}$, where the Schrieffer-Wolff transformation allow us to get the following Hamiltonian

$$\langle\alpha|H_{\text{eff}}^{00}|\alpha'\rangle = - \sum_j P_j (I_j^z)^2 + \frac{1}{2} \sum_{\alpha''\beta''} \langle 00, \alpha | \sum_j H_j^{(e-n)} | \beta'' \alpha'' \rangle \langle \beta'' \alpha'' | \sum_k H_k^{(e-n)} | 00, \alpha' \rangle \left(\frac{1}{\omega_{\alpha\alpha''} + \omega_{\beta\beta''}} + \frac{1}{\omega_{\beta\beta''} + \omega_{\alpha'\alpha''}} \right), \quad (11)$$

where the energy zero is shifted to $E_0 = \sum_j \frac{2}{3}(P_j - D_j)$, and one has to sum over all the electronic states $\{|\beta''\rangle\}$ on the first-excited manifold in Fig. 1(b). There are thus two types of channels of virtual electron spin flips, and these correspond to the symmetric $|\mathbb{S}_\pm\rangle = (|0, \pm 1\rangle_e + |\pm 1, 0\rangle_e)/\sqrt{2}$, and anti-symmetric $|\mathbb{A}_\pm\rangle = (|0, \pm 1\rangle_e - |\pm 1, 0\rangle_e)/\sqrt{2}$ combinations. Due to the dipole-dipole interaction, these channels are split in energies by $E_s - E_a = 2J_{12}$, which is the key ingredient that allow us to obtain a non-vanishing interaction between the nuclear spins. By expanding to leading order for $\beta'' = \mathbb{S}_\pm, \mathbb{A}_\pm$, we obtain $(\omega_{\alpha\alpha''} + \omega_{00\beta''})^{-1} \approx \omega_{00\beta''}^{-1} \approx D^{-1}(1 \mp J_{12}/D)$ for the symmetric/anti-symmetric states. By resumming the expression above, one finally arrives to the effective nuclear Hamiltonian, which reads

$$H_{\text{eff}}^{00} = -\sum_j P_j (I_j^z)^2 + J_{\text{eff}}^{\text{xx}} (I_1^+ I_2^- + I_1^- I_2^+), \quad (12)$$

where $J_{\text{eff}}^{\text{xx}} = 2A_1^\perp A_2^\perp J_{12}/D^2$, and we have a negligible local energy shift for $(A_j^\perp)^2/D \ll D$. This is precisely the spin-spin Hamiltonian $H_{\text{eff}}^{\text{xx}}$ described in Eq. (3), which leads to the exchange of spin excitations between the nuclei. Let us finally remark that in this derivation we have assumed that there is no inhomogeneous broadening $D_1 = D_2$, which may modify the results. However, since the effective interactions are so weak $J_{\text{eff}}^{\text{xx}} \approx 0.1\text{Hz}$, there is no point of being more rigorous at this point. In the next section, we shall treat the possible effects of inhomogeneous broadening for the driven interactions in detail.

Effective nuclear Hamiltonian for the driven regime.- In this part of the Appendix, we discuss the RWA leading to Eq. (5), and the Schrieffer-Wolff transformation to the effective nuclear Hamiltonian in Eq. (6).

a) Driven Hamiltonian.- Let us rewrite the total driven Hamiltonian in Eqs. (1),(2), and (4) as follows $H = H_{0,1} + H_{0,2}$, where

$$\begin{aligned} H_{0,1} &= \sum_j D_j (S_j^z)^2 + g_e \mu_B B \cos \theta_j S_j^z - P_j (I_j^z)^2 - g_n \mu_N B \cos \theta_j I_j^z, \\ H_{0,2} &= \sum_j \frac{1}{2} B \sin \theta_j (g_e \mu_B e^{-i\varphi_j} S_j^+ - g_n \mu_N e^{-i\varphi_j} I_j^+ + \text{H.c.}) + \sum_j H_j^{(e-n)} + H_{12}^{(e-e)} + H_d(t), \end{aligned} \quad (13)$$

where we again shifted the energy zero to $E_0 = \sum_j \frac{2}{3}(P_j - D_j)$, and we have introduced the relative orientation of the NV centers (θ_j, φ_j) with respect to the applied magnetic fields. In the interaction picture $H_{0,2}(t) = e^{iH_{0,1}t} H_{0,2} e^{-iH_{0,1}t}$, one can neglect rapidly oscillating terms by a rotating wave approximation (RWA), which leads us to

$$H_{0,2}^{\text{rwa}} \approx \sum_j \left(\frac{1}{2} \Omega_e \sigma_j^x + \frac{1}{2} \Omega_n \tau_j^x \right) + 2J_{12} S_1^z S_2^z + \sum_j A_j^\parallel S_j^z I_j^z, \quad (14)$$

where we define $B_j = B \cos \theta_j$. This RWA is justified when $D_j \gg g_e \mu_B B_j \gg \Omega_e, A_j^\perp, P_j \gg g_n \mu_B B \gg \Omega_n$, which is clearly fulfilled for the parameters shown in Table I. Additionally, the inhomogeneous splitting allows us to neglect the transverse part of the magnetic dipole coupling between the electron spins $J_{12} \ll g_e \mu_B |B_1 - B_2|$. According to Table I, one can neglect these terms $A_j^\perp/D_j \sim 10^{-3}$, $g_e \mu_B B/D_j \sim 10^{-2}$, $\Omega_e/g_e \mu_B B \sim 10^{-1}$, $g_n \mu_N B/P_j \sim 10^{-3}$, $\Omega_n/g_n \mu_N B \sim 10^{-1}$. Besides, for two NV centers oriented along different axes, $\theta_1 - \theta_2 \sim \mathcal{O}(\pi)$, we can neglect the transverse dipole-dipole coupling $J_{12}/g_e \mu_B |B_1 - B_2| \sim 10^{-3}$.

In order to confirm the validity of these approximations, we must compare the dynamics of both Hamiltonians, $H_{0,2}(t), H_{0,2}^{\text{rwa}}$. Let us note that the full time-dependent Hamiltonian $H_{0,2}(t) = e^{iH_{0,1}t} H_{0,2} e^{-iH_{0,1}t}$ contains very different time-scales, ranging from ns to ms . To reproduce the dynamics faithfully, one sets the numerical integration time-step to the smallest time-scale, ns . For such a small time-step, prohibitively large integration times are required in order to reach the ms -regime where the nuclear spin-spin interaction effects become visible. Nonetheless, to test the accuracy of the RWA, it suffices to study $t \in [0, 2\pi/A_j^\parallel]$, which lies in the μs -range. In Fig. 3(a), we compare both predictions numerically for the initial state $|\psi_0\rangle = |--\rangle_e \otimes |-\rangle_n$, namely

$$\langle \tau_j^x(t) \rangle_{\text{rwa}} = \langle \psi_0 | e^{iH_{0,2}^{\text{rwa}}t} \tau_j^x e^{-iH_{0,2}^{\text{rwa}}t} | \psi_0 \rangle, \quad \langle \tau_j^x(t) \rangle_{\text{exact}} = \langle \psi_0 | e^{i \int_0^t dt' H_{0,2}(t')} \tau_j^x e^{-i \int_0^t dt'' H_{0,2}(t'')} | \psi_0 \rangle. \quad (15)$$

Since there is no refocusing echo pulse, the nuclear spin dynamics should be dominated by the Rabi oscillations caused by the term $-\frac{1}{4} A_j^\parallel \tau_j^z$ in Eq. (6). As observed in Fig. 3(a), these neat μs Rabi flops display a perfect agreement between the exact Hamiltonian and the RWA approximation.

b) Effective nuclear Hamiltonian: According to the preceding discussion, we shall consider directly the RWA Hamiltonian in Eq. (5), where the set of Pauli matrices is defined as follows

$$\begin{aligned} \sigma_j^z &= |0_j\rangle_e \langle 0_j|_e - |1_j\rangle_e \langle -1_j|_e, \quad \sigma_j^x = |-1_j\rangle_e \langle 0_j|_e + \text{H.c.} \\ \tau_j^z &= |0_j\rangle_n \langle 0_j|_n - |1_j\rangle_n \langle -1_j|_n, \quad \tau_j^x = |-1_j\rangle_n \langle 0_j|_n + \text{H.c.} \end{aligned} \quad (16)$$

and the sub-indexes $|\rangle_e, |\rangle_n$ indicate the electronic or nuclear origin of the spin state. In this two-level approximation, the spin-1 operators become $S_j^z = |1_j\rangle_e \langle 1_j|_e + \frac{1}{2}(\sigma_j^z - \mathbb{I}_2)$, and $I_j^z = |1_j\rangle_n \langle 1_j|_n + \frac{1}{2}(\tau_j^z - \mathbb{I}_2)$. Accordingly, the electronic and nuclear

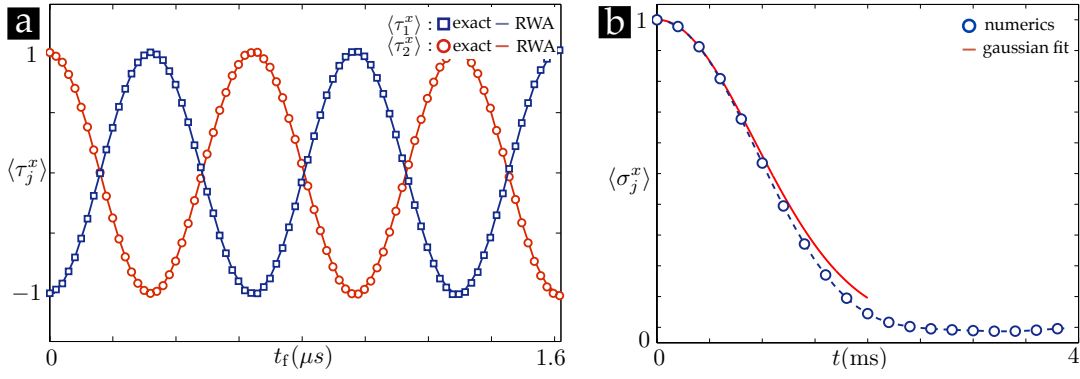


Figure 3. **Rotating wave approximation and free induction decay.** (a) Accuracy of the rotating wave approximation: Dynamics of the expectation values $\langle \tau_j^x(t) \rangle_{\text{rwa}}$ (squares, circles), as solved by numerical exponentiation, and $\langle \tau_j^x(t) \rangle_{\text{exact}}$ (solid lines), as solved numerically by a fourth order Runge-Kutta method. (b) Free induction decay due to magnetic noise: Numerical simulation of the stochastic dynamics of the free induction decay $\langle \tau_x(t) \rangle$ (circles), for the initial state $|\Psi_0\rangle = (|0\rangle_e + |-1\rangle_e)/\sqrt{2}$, after averaging for $N_{\text{it}} = 5 \cdot 10^3$ trajectories of the random process (25). The red line corresponds to a gaussian fit $\langle \tau_x(t) \rangle_{\text{fit}} \propto \exp(-\frac{1}{2}b_{\text{fit}}^2 t^2)$, where $b_{\text{fit}} = 1.09\text{kHz}$.

levels $m_j = 1, M_j = 1$ decouple, and one may write the following driven pseudospin-1/2 Hamiltonian

$$H_0 = \sum_j \left(\frac{1}{2} \Omega_e \sigma_j^x + \frac{1}{2} \Omega_n \tau_j^x \right) + \frac{1}{2} J_{12} (\sigma_1^z - \mathbb{I}_2) (\sigma_2^z - \mathbb{I}_2), \quad H_1 = \sum_j \frac{1}{4} A_j^{\parallel} (\sigma_j^z - \mathbb{I}_2) (\tau_j^z - \mathbb{I}_2), \quad (17)$$

Once the pseudospin-1/2 Hamiltonian in Eq. (17) has been derived, we adiabatically eliminate the fast electronic degrees of freedom from the slow nuclear dynamics by a Schrieffer-Wolff transformation. We shall make use of Eq. (10), where we identify $\beta = \{-, -\}$ as the lowest-energy manifold (see Fig. 1(d)), $\beta'' = \text{S, A}$ as the symmetric/anti-symmetric excited manifolds

$$|\text{S}\rangle = \frac{1}{\sqrt{1+(1+\xi)^2}} ((1+\xi)|+-\rangle_e + |-+\rangle_e), \quad |\text{A}\rangle = \frac{1}{\sqrt{1+(1-\xi)^2}} ((1-\xi)|+-\rangle_e - |-+\rangle_e), \quad (18)$$

where we have introduced $|\pm\rangle_e = (|0\rangle_e \pm |-1\rangle_e)/\sqrt{2}$, and a parameter $\xi \ll 1$ quantifying the inhomogeneous broadening $A_1^{\parallel} \neq A_2^{\parallel}$. These levels are split in energies by $2J(\xi)$, where

$$J(\xi) = \frac{J_{12}}{2} \sqrt{1+\xi^2}, \quad \xi = \frac{2}{\Omega_e J_{12}} [(A_2^{\parallel})^2 - (A_1^{\parallel})^2], \quad (19)$$

To second order in the hyperfine coupling, we are able to derive

$$H_{\text{eff}}^- = \sum_j (\Omega_n \tau_j^x + \frac{1}{4} A_j^{\parallel} \tau_j^z) - \frac{1}{16 \Omega_{\text{eS}}} \langle -- | \sum_j A_j^{\parallel} \sigma_j^z \tau_j^z | \text{S} \rangle \langle \text{S} | \sum_k A_k^{\parallel} \sigma_k^z \tau_k^z | -- \rangle - \frac{1}{16 \Omega_{\text{eA}}} \langle -- | \sum_j A_j^{\parallel} \sigma_j^z \tau_j^z | \text{A} \rangle \langle \text{A} | \sum_k A_k^{\parallel} \sigma_k^z \tau_k^z | -- \rangle, \quad (20)$$

where we have introduced the following energy differences

$$\Omega_{\text{eS}} = \Omega_e \left[1 + \left(\frac{A_1^{\parallel}}{\Omega_e} \right)^2 + \left(\frac{A_2^{\parallel}}{\Omega_e} \right)^2 \right] + J(\xi), \quad \Omega_{\text{eA}} = \Omega_e \left[1 + \left(\frac{A_1^{\parallel}}{\Omega_e} \right)^2 + \left(\frac{A_2^{\parallel}}{\Omega_e} \right)^2 \right] - J(\xi). \quad (21)$$

By computing the corresponding matrix elements, together with a Taylor expansion for $\Omega_e \gg A_j^{\parallel}, J_{12}$, and $1 \gg \xi$, we find the following expression for the followig nuclear spin Hamiltonian, which is precisely Eq. (6) in the main text,

$$H_{\text{eff}}^- = J_{\text{eff}}^{zz} \tau_1^z \tau_2^z + \sum_j \Omega_n \tau_j^x - \frac{1}{4} A_j^{\parallel} \tau_j^z, \quad J_{\text{eff}}^{zz} = \frac{-A_1^{\parallel} A_2^{\parallel}}{8 \Omega_e} \left(\frac{J_{12}}{\Omega_e} + 2\xi \right), \quad (22)$$

2. Decoherence and effective decoupling by continuous microwave driving

In order to perform quantum-information tasks in a solid-state device, the effects of the system-environment coupling must be carefully addressed. In contrast to cold-atom platforms, the environment in a solid is rather complex since the spins may couple to a wide variety of excitations. In the case of NV centers, whose energy levels lie deep in the band gap of diamond, the major

source of noise is the coupling to the spins of different impurities, rather than to electronic or vibronic excitations. Accordingly, one should consider the effects of a spin bath on the coherent features of the electron/nuclear spin of the NV center.

Phenomenological magnetic noise model.- The problem of a central spin coupled to an ensemble of bath spins has been studied since the early days of nuclear magnetic resonance [5], and depending on the particular nature of the spin bath can be an intricate many-body problem. For type Ib diamond, the bath consists of the electronic spins of ^{14}N impurities, the so-called P1 centers, randomly distributed through the sample. The dipolar coupling of the P1 centers to the NV electron spin gives rise to a pure dephasing which can be treated by mean-field theories [21]. Conversely, for ultrapure type IIa diamond, it is the nuclear spin of ^{13}C isotopes which yields the dephasing of the NV center via the hyperfine electron-nuclei coupling [8]. Interestingly, the correlations of this nuclear-spin environment must be accounted in order to reproduce the short-time dynamics of the system. In this work, we follow a phenomenological approach rather than a microscopic one, where the magnetic noise is modeled by a random fluctuation of the resonance frequencies associated to the electron/nuclear spins. This model captures the whole dynamics of type Ib diamond [19], and is expected to describe faithfully the long-time dynamics of type IIa diamond ($t_f \sim \text{ms}$), where the non-Markovian aspects of the environment should not have an important effect.

The flip-flop interactions between the NV and the bath spins can be safely neglected due to their utterly different energy scales. Therefore, we consider that the collective effect of the spin bath is to shift the resonance energies of the NV center (i.e. pure dephasing), which can be modeled by an effective local magnetic field. In order to account for the spin-bath dynamics, this magnetic field is treated as a stochastic process [19]. Hence, the NV centers are described by a stochastic Hamiltonian

$$H(\{b_j(t), B_j(t)\}) = \sum_j \left(H_j^{(e)} + H_j^{(n)} + H_j^{(e-n)} \right) + H_{12}^{e-e} + H_d(t) + H_{\text{noise}}, \quad H_{\text{noise}} = \sum_j \left(b_j(t) S_j^z + B_j(t) I_j^z \right), \quad (23)$$

where $b_j(t), B_j(t)$ are the random processes describing the fluctuating resonance frequencies. Whereas the electron and nuclear spins of the NV center follow the unitary dynamics dictated by the Schrödinger equation $i\partial_t |\Psi\rangle = H(\{b_j(t), B_j(t)\}) |\Psi\rangle$, the fluctuating fields evolve according to the so-called Langevin equation $d_t X(t) = A(X(t), t) X(t) + \sqrt{D(X(t), t)} \Gamma(t)$, where $X(t) = \{b_j(t), B_j(t)\}$ is the random process, $A(x, t)$, and $D(x, t) > 0$, are smooth functions, and $\Gamma(t)$ is a Gaussian zero-mean noise (i.e. $\langle \Gamma(t) \rangle = 0$, $\langle \Gamma(t) \Gamma(t') \rangle = \delta(t - t')$) [6]. Due to the large number of spins conforming the bath, these random processes can be argued to be *Gaussian* by means of the central limit theorem. Besides, when the back-action of the system is small [19], or we are interested in the long-time dynamics, the process can be treated as *Markovian* and *stationary*. In this case, one obtains a Langevin equation with $A(x, t) = -x/\tau$, and $D(x, t) = c$, where τ is the relaxation time of the process, and c the diffusion speed. The solution to this equation can be obtained explicitly, and is known as the *Ornstein-Uhlenbeck* (OU) process [7]. In the case of zero-mean random magnetic fields, the auto-covariances are

$$\langle b_j(t) b_j(0) \rangle = b_j^2 e^{-r_j t}, \quad \langle B_j(t) B_j(0) \rangle = B_j^2 e^{-R_j t}, \quad (24)$$

where $b_j^2 = \frac{1}{2} c b_j \tau_{b_j}$, $B_j^2 = \frac{1}{2} c B_j \tau_{B_j}$ represent the variances of the zero-mean gaussian distributions, and $r_j = 1/\tau_{b_j}$, $R_j = 1/\tau_{B_j}$ the inverse of their relaxation times. These auto-correlations lead to a Lorentzian spectral density, which contains a white-noise region at low frequencies, and $1/f^2$ -noise region at larger frequencies. Interestingly enough, the dynamics of the OU process can be given explicitly [7], and numerical integration of the Langevin equation is not required. In fact, for any discretization $dt > 0$, one finds the following exact update formula

$$X(t + dt) = X(t) e^{-t/\tau} + \sqrt{\frac{c\tau}{2} (1 - e^{-2dt/\tau})} n, \quad (25)$$

where n is a zero-mean unit-variance gaussian random variable which is time uncorrelated. In order to solve the whole stochastic quantum dynamics in Eq. (24), we discretize the time interval in M time-steps, $t_m = mdt \in [0, t_f]$, where $dt = t_f/M$, and obtain the different values of the fluctuating magnetic fields $b_j(t_m), B_j(t_m)$ by employing the above formula (25). Then, we integrate numerically the stochastic Hamiltonian for the particular sampling of the random process $s = \{b_j(t_m), B_j(t_m)\}$, and recover the expectation values $\langle \tau_j^x \rangle_s$. By repeating this procedure for $N_{\text{it}} \gg 1$, one can perform the statistical average over the stochastic noise, $\langle \tau_j^x \rangle = \frac{1}{N_{\text{it}}} \sum_s \langle \tau_j^x \rangle_s$, and thus study the effects of the decoherence.

To illustrate the physics of this phenomenological model, let us consider the simpler situation of a single NV electron spin. We consider the decoherence of a Ramsey experiment, where the initial state corresponds to $|\Psi_0\rangle = (|0\rangle_e + |-1\rangle_e)/\sqrt{2}$, and we measure the so-called free induction decay (FID) due to the noise after a certain time t , $\langle \sigma^x(t) \rangle$. In Fig. 3(b), we represent the time evolution of the FID derived from the numerical solution of the stochastic Hamiltonian $H(b(t)) = b(t) S^z$, where $b(t)$ is a OU process with $b = 1\text{kHz}$, and we have averaged over $N_{\text{it}} = 5 \cdot 10^3$ samplings of the random process. Due to the magnetic noise, the free induction decay follows a gaussian decay law $\langle \tau_x(t) \rangle \propto \exp(-\frac{1}{2} b^2 t^2)$, which allows us to identify the dephasing time as $T_{2,e} = 1/b \approx 1\text{ms}$. Therefore, we observe how the phenomenological noise model allows us to study the decoherence effects for different dephasing rates, which has been used in the main text (Fig. 2(e)).

Effective decoupling mechanisms.- An advantage of the phenomenological noise models is that they allow a neat understanding of the effects of decoherence, together with possible strategies to overcome them. In the particular case of the driven

Hamiltonian (5), it is easy to observe that the fluctuation of the electronic resonance frequencies, $H = \sum_j b_j(t) S_j^z$, tries to induce transitions between the energy manifolds of Fig. 1(d), namely $|+j\rangle_e \leftrightarrow |-j\rangle_e$. However, since these states now have a huge energy difference given by the Rabi frequency of the driving Ω_e , these transitions are non-resonant and thus partially suppressed. In fact, the electron magnetic noise can only couple to the nuclei via second order processes. The leading order contribution comes from the coupling to the hyperfine channel, and gives rise to $H_{\text{eff}} \approx \sum_j (b_j A_j^{\parallel} / \Omega_e) \tau_j^z$, which is partially suppressed for the regime considered in this work $b_j, A_j \ll \Omega_e$. Now, one has to compare this new term to the nuclear driving, and since $(b_j A_j^{\parallel} / \Omega_e) \ll \Omega_n$, we get an additional decoupling mechanism. Qualitatively, one can argue that the effects of the noise give rise to a small second-order fluctuation of the nuclear driving $H_{\text{eff}} \approx \sum_j \Omega_n (1 + \frac{1}{2} (b_j A_j^{\parallel} / \Omega_e)^2 / \Omega_n^2) \tau_j^x$. In this expression, one observes the two-fold role of the microwave driving Ω_e . On the one hand, Ω_e must be small enough so as to increase the effective nuclear interaction. On the other hand, Ω_e must be big enough so as to provide an effective decoupling from the electronic noise. Therefore, one must find a compromise between the two, such as that presented for the parameters in Table I. With respect to the additional decoupling due to the driving of the nuclei, Ω_n must be as big as possible. By increasing the external magnetic fields beyond $B \approx 500\text{G}$, where the levels $m_j = 0, -1$ become degenerate, one could raise the nuclear driving strength, and thus increment the efficiency of the decoupling.

-
- [1] C. Cohen-Tannoudji, J. Dupont-Roc and G. Grynberg, *Atom- Photon Interactions*, (Wiley-VCH, Weinheim, 2004).
 - [2] J. R. Schrieffer and P. A. Wolff, *Phys. Rev.* **149**, 491 (1966).
 - [3] R. Winkler, in *Spin-Orbit Coupling Effects in Two-Dimensional Electron and Hole Systems*, (Springer-Verlag, Berlin, 2003).
 - [4] J. H. Van Vleck, *Phys. Rev.* **33**, 467 (1929); L.L. Foldy and S. A. Whouthuysen, *Phys. Rev.* **78**, 29 (1950); J. M. Luttinger and W. Kohn, *Phys. Rev.* **97** 869 (1955).
 - [5] P. W. Anderson and P. R. Weiss, *Rev. Mod. Phys.* **25**, 269 (1953).
 - [6] N. G. Van Kampen, *Stochastic Processes in Physics and Chemistry*, (North-Holland, Amsterdam, 1981).
 - [7] D. T. Gillespie, *Am. J. Phys.* **64**, 3 (1996).
-